Solid-State Electronics 200 (2023) 108549

Contents lists available at ScienceDirect

Solid State Electronics

journal homepage: www.elsevier.com/locate/sse

Comparative analysis of NBTI modeling frameworks BAT and Comphy☆

Aseer Israr Ansari *, Nilotpal Choudhury, Narendra Parihar, Souvik Mahapatra

Department of Electrical Engineering, Indian Institute of Technology Bombay, Mumbai, 400076, Maharashtra, India

ARTICLE INFO

Keywords:
NBTI modeling
BAT
Comphy

ABSTRACT

The Compact-Physical (Comphy) framework is tested against the experimental Negative Bias Temperature Instability (NBTI) data. A cost-function based optimizer is used for obtaining the parameters of Comphy. The ultrafast (10 μs delay) measured threshold voltage shift (ΔV_T) during and after NBTI stress at various stress (V_{GSTR}) and recovery (V_{GREC}) bias, temperature (T) and stress time (t_{STR}), and mixed AC–DC stress using random V_{GSTR}, V_{GREC}, pulse duty cycle (PCD) and frequency (f) are used to test the model framework. The BTI Analysis Tool (BAT) framework, for which data from previous work is used, and Comphy are compared.

1. Introduction

NBTI continues as a dominant reliability issue in modern p-FETs [1–5]. It causes positive charge buildup in the gate insulator of the device during stress, and shifts its parameters in time. The accrued charges partially reduce after the removal of stress, which results in recovery of parametric shift. Therefore, the modeling of NBTI becomes challenging, especially for gate pulses having arbitrary on (stress) and off (recovery) phases that mimic the data-paths in digital circuits, and for non-digital pulses encountered in analog and mixed-signal applications.

Although the physics of NBTI remains debated [6–8], there are two competing frameworks at present: BAT [1] and Comphy [9], the latter is publicly available in [10]. Both the frameworks have physics based models. In BAT, uncorrelated contributions from interface trap generation (ΔV_{IT}), trapping of holes in pre-existing traps (ΔV_{HT}), and generation of bulk gate insulator traps (ΔV_{OT}) are used to model the ΔV_T time kinetics during and after stress (Fig. 1). On the other hand, Comphy uses uncorrelated contributions from the recoverable (R) and (semi) permanent (P) components. In modern p-FETs having High-K Metal Gate (HKMG) stacks, R is individually calculated for the interlayer (IL) and High-K layer (Fig. 2).

BAT is successfully validated by using diverse experimental conditions and across various technologies [1,11,12]. In this work, the Comphy framework is evaluated using basic DC stress-recovery and mixed DC–AC stress. The BAT results from [1] are shown as a comparative reference.

2. BAT

In BAT (Fig. 1), the ΔV_T time kinetics is obtained from three uncorrelated components, interface trap generation (ΔV_{IT}), trapping of holes in pre-existing traps (ΔV_{HT}), and generation of bulk gate insulator traps (ΔV_{OT}). Reaction–Diffusion (RD) model together with Transient Trap Occupancy Model (TTOM) is used for ΔV_{IT}, Activated Barrier Double Well Thermionic (ABDWT) model for ΔV_{HT}, and Reaction–Diffusion–Drift (RDD) model for ΔV_{OT}, the model details and parameters are provided in various chapters of [1].

The RD model has a total of 17 parameters of which, only 4 are varied to match the measured data, TTOM has 8 parameters of which 2 are varied, ABDWT has 9 parameters of which 4 are varied and RDD has 16 parameters of which 4 are varied. In total, there are 14 variable parameters. For this work, the values of these parameters are taken from [1].

3. Comphy

In Comphy (Fig. 2), the ΔV_T time kinetics is obtained from two uncorrelated components, the recoverable (R) and (semi) permanent (P) components. The recoverable component is handled by two Non-radiative Multi-Phonon (NMP) models, one for each layer of oxide, and the permanent component is handled by the Two Well Thermionic (TWT) model. The model details are provided in [9].

Each NMP model has total 6 parameters. The TWT model has total 7 parameters. This adds up to a total of 19 parameters. A Root Mean Square Error (RMSE) cost function based optimizer is used to

☆ The review of this paper was arranged by Francisco Gamiz.

* Corresponding author.
E-mail addresses: aseerisrar@gmail.com (A.I. Ansari), nilotpal.nits@gmail.com (N. Choudhury), np.electro@gmail.com (N. Parihar), souvik@ee.iitb.ac.in (S. Mahapatra).

https://doi.org/10.1016/j.sse.2022.108549

Available online 5 December 2022

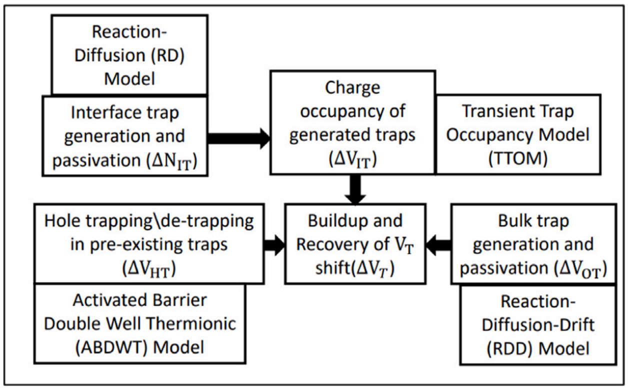

Fig. 1. Schematic of BAT Framework.

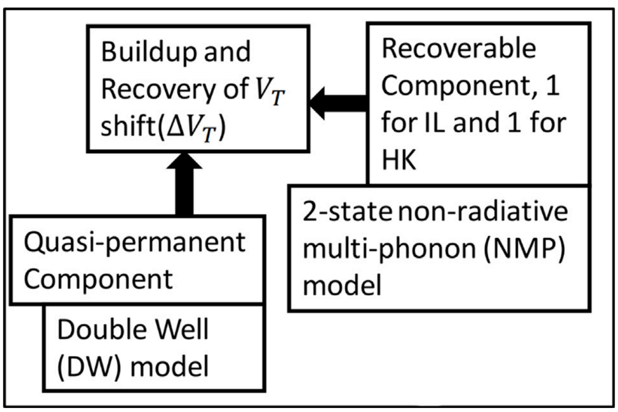

Fig. 2. Schematic of Comphy Framework.

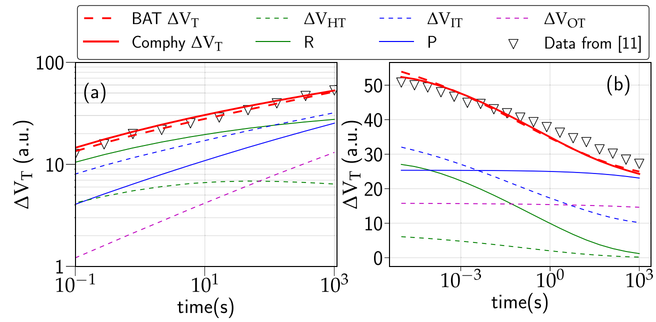

Fig. 3. Measured (symbols) and modeled (lines) ΔV_T time evolution at fixed V_{GSTR} = −1.7 V and T = 100 °C during (a) stress and (b) subsequent recovery in RMG FinFET.

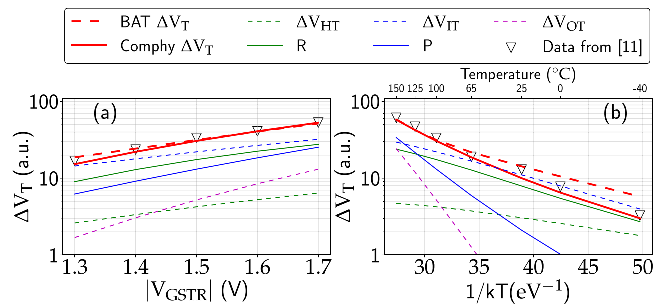

Fig. 4. Measured (symbols) and modeled (lines) fixed time ΔV_T at t_{STR} = 1 Ks, as a function of (a) V_{GSTR} at T = 100 °C, (b) *T* at V_{GSTR} = −1.5 V. in RMG FinFET.

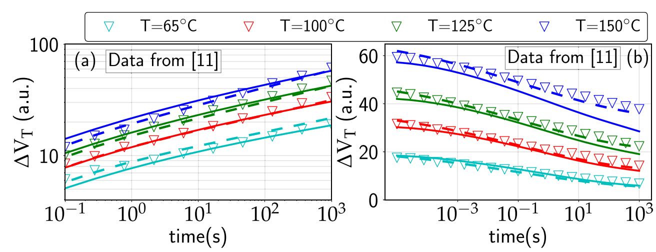

Fig. 5. Measured (symbols) and modeled (lines) ΔV_T time evolution at fixed V_{GSTR} = −1.5 V for different *T* during (a) stress and (b) subsequent recovery in RMG FinFET. Solid and Dashed lines are for Comphy and BAT respectively.

fit Comphy simulation with measured data, and all 19 parameters are freely varied. Once a set of optimal parameters is obtained for a particular device, they are kept fixed to simulate different experimental conditions.

4. Experiments

4.1. RMG FinFET

Measurements from Replacement Metal Gate (RMG) HKMG p-FinFETS [11] fabricated using proprietary IBM SOI process are used in this paper. These devices have 20-nm channel length, the number of fins is 42 to reduce variability. The gate stack has the standard chemical oxide-based interlayer (IL), hafnium oxide-based high-k and low nitrogen (N) content in the IL, and has an equivalent oxide thickness of 1 nm.

The parameters of BAT for RMG FinFET are taken from [1]. The parameters for Comphy are obtained by fitting simulation results with the measured ΔV_T time kinetics at different V_{GSTR} and T. The minimize function in the scipy library of python is used for obtaining the parameters. The RMSE cost function and Nelder–Mead method is used for optimization. The Comphy parameters are listed in Table 1.

Measured ΔV_T time kinetics (at fixed V_{GSTR}, T) and fixed time ΔV_T versus V_{GSTR} and *T* from RMG HKMG FinFETs are modeled respectively in Figs. 3 and 4 by BAT and Comphy, and the corresponding subcomponents are also shown. For BAT, during stress, ΔV_{HT} saturates early, while ΔV_{IT} and ΔV_{OT} evolve in time, respectively with long-time power-law slope of ∼ 1/6 and ∼ 1/4; after stress, ΔV_{HT} and ΔV_{OT} respectively recover fast and show negligible recovery, while ΔV_{IT} recovers over an extended period; ΔV_{IT} dominates overall ΔV_T (unless at high V_{GSTR} and/or T). For Comphy, during stress, R evolves with a shallower time slope than P, while recovery is only due to R; equal contribution is made by R and P (unless at high *T* when P dominates). For the same device, measured and modeled ΔV_T time kinetics during and after stress at fixed V_{GSTR} and varying *T* (Fig. 5), and at fixed *T* and varying V_{GSTR} (Fig. 6), and fixed time ΔV_T versus V_{GSTR} at various *T* (Fig. 7) are shown. These parameters are then used to model recovery kinetics at different t_{STR} (Fig. 8), and different V_{GREC} (Fig. 9). The figures are made in arbitrary units (a.u.) to maintain confidentiality of the data.

4.2. GF planar MOSFET

Measurements from Gate First (GF) HKMG planar p-MOSFETs [12] with ultrathin thermal interlayer (IL) are used. The device have IL of thickness 2.4 Å(N-based IL) and high-k of effective oxide thickness of 4.6 Å.

The parameters of BAT for GF Planar MOSFET are taken from [1]. For Comphy, two sets of (19) parameters are obtained, by fitting only ΔV_T stress-recovery time kinetics (DC optimized, Fig. 10) and also considering DC multicycle data (Total optimized, Figs. 11 and

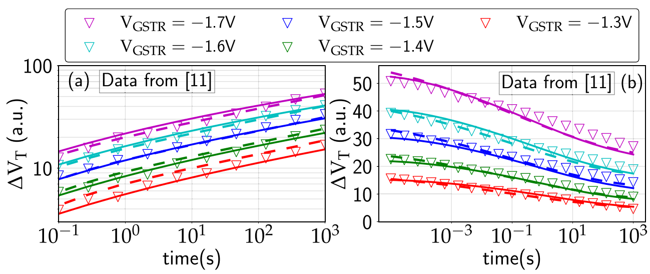

Fig. 6. Measured (symbols) and modeled (lines) ΔV_T time evolution at fixed T = 100 °C for different V_{GSTR} during (a) stress and (b) subsequent recovery in RMG FinFET devices. Solid and Dashed lines are for Comphy and BAT respectively.

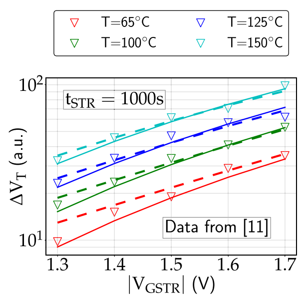

Fig. 7. Fixed time ΔV_T as a function of V_{GSTR}, in RMG FinFET. Solid and Dashed lines are for Comphy and BAT respectively.

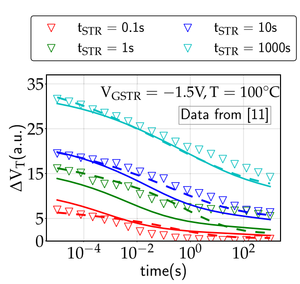

Fig. 8. ΔV_T time evolution with different t_{STR} in RMG FinFET. Solid and Dashed lines are for Comphy and BAT respectively.

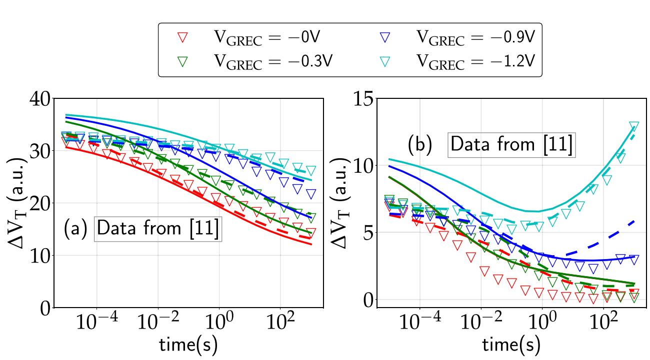

Fig. 9. Measured (symbols) and modeled (lines) ΔV_T time evolution at fixed V_{GSTR} = −1.5 V and T = 100 °C but different V_{GREC} in RMG FinFET for (a) t_{STR} =1000 s, (b) t_{STR}=0.1 s. Solid and Dashed lines are for Comphy and BAT respectively.

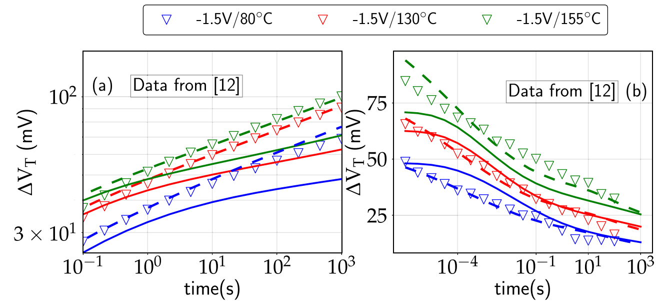

Fig. 10. Measured (symbols) and modeled (lines) ΔV_T time evolution during (a) stress and (b) subsequent recovery in GF planar MOSFET, with DC optimized parameters for Comphy. Solid and Dashed lines are for Comphy and BAT respectively.

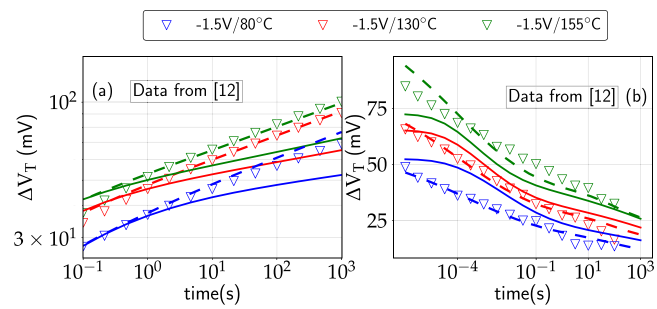

Fig. 11. Measured (symbols) and modeled (lines) ΔV_T time evolution during (a) stress and (b) subsequent recovery in GF planar MOSFET, with Total optimized parameters for Comphy. Solid and Dashed lines are for Comphy and BAT respectively.

Table 1
Comphy Parameters obtained from the optimizer fpr both the devices. NMP-1 is the NMP model in High-k, and NMP-2 is the NMP model in SiO2. Some parameters for RMG FinFET are hidden to maintain confidentiality of the data.

Model	Parameters	RMG FinFET	GF planar MOSFET	
			DC optimized	Total optimized
NMP-1	$\langle E_T \rangle$ (eV)	−1.18	−0.815	−0.826
	σ_{E_T} (eV)	–	0.637	0.604
	$\langle S \rangle$ (eV)	9.83	2.81	3.22
	σ_S (eV)	1.62	1.32	1.18
	R	1.1	0.764	0.825
	N_T (cm^{-3})	–	7.25×10^{22}	8.79×10^{22}
NMP-2	$\langle E_T \rangle$ (eV)	−1.12	−0.931	−0.917
	σ_{E_T} (eV)	–	0.09	0.08
	$\langle S \rangle$ (eV)	4.27	3.4	3.24
	σ_S (eV)	1.71	0.8	0.76
	R	1.56	1.58	1.62
	N_T (cm^{-3})	–	2.26×10^{23}	2.26×10^{23}
TWT	$\langle \epsilon_1 \rangle$ (eV)	2.18	3.08	2.77
	σ_{ϵ_1} (eV)	–	0.73	0.81
	$\langle \epsilon_2 \rangle$ (eV)	2.36	3.44	3.37
	σ_{ϵ_2} (eV)	0.467	0.25	0.24
	k_0 (s^{-1})	2.18×10^{13}	8.03×10^{10}	7.67×10^{10}
	γ (eV m/V)	6.56×10^{-10}	1.7×10^{-9}	1.58×10^{-9}
	N_T (cm^{-2})	–	2.66×10^{17}	3.17×10^{17}

12(a)&(b)). The parameters are obtained in the same way as before, by using the minimize function of the scipy library in python with a RMSE cost function. The Nelder–Mead method is used for optimization. The Comphy parameters are listed in Table 1.

DC multicycle simulation (Fig. 12(a)&(b)) are shown for both sets of parameters. The Total optimized parameters are then used for simulation of mixed DC–AC in Figs. 12(c)–(f) and 13(a)–(b), and AC multicycle with different V_{GHIGH}, f and PDC in Fig. 13(c)–(f).

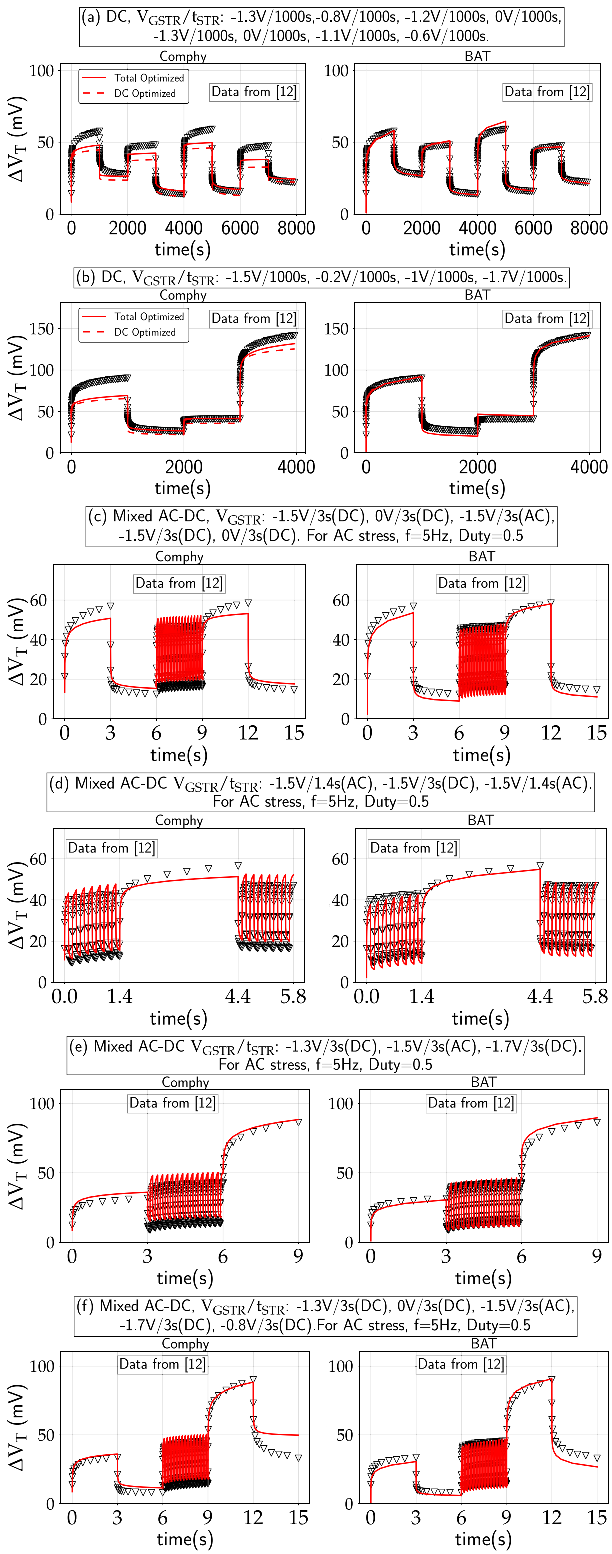

Fig. 12. Measured (symbols) and modeled (lines) of arbitrary ΔV_T in GF planar MOSFET (a) & (b) multiple dc segments with different V_{GSTR} but fixed t_{STR}, (c) mixed ac–dc stress with inserted recovery after dc stress and fixed V_{GSTR} and t_{STR}, (d) mixed ac–dc stress with ac stress before dc stress and fixed V_{GSTR}, (e) mixed ac–dc stress with ac between dc stress and varying V_{GSTR}, (f) mixed ac–dc stress with inserted recovery after dc stress and varying V_{GSTR}.

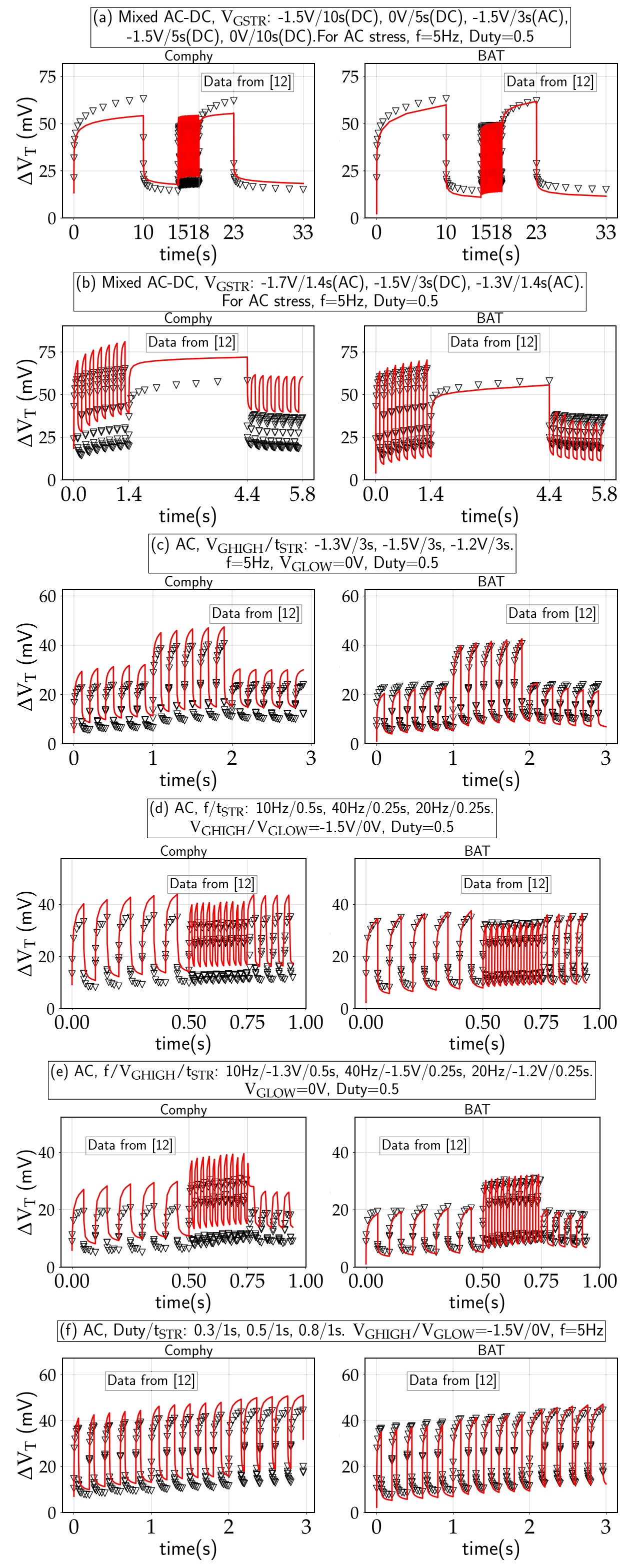

Fig. 13. Measured (symbols) and modeled (lines) of arbitrary ΔV_T in GF planar MOSFET (a) mixed ac–dc stress with inserted recovery after dc stress with fixed V_{GSTR} and varying t_{STR}, (b) mixed ac–dc stress with ac stress before dc stress with varying V_{GSTR} and t_{STR} (c) multiple ac stress with varying V_{GHIGH}, (d) multiple ac stress with varying frequency, (e) multiple ac stress with varying V_{GHIGH} and frequency, (f) multiple ac stress with varying PDC.

5. Conclusion

BAT and Comphy can model simple time kinetics during and after NBTI stress at different $V_{GSTR} \times T$. However, Comphy faces some challenges in modeling recovery at different V_{GREC} (for analog applications), as well as arbitrary and mixed DC–AC gate waveforms (for digital data-path signals), although BAT can model the same. For GF Planar MOSFET, in order for the recovery to work, the stress end values are being underestimated which is not the case in BAT. This can be attributed to the TTOM model in BAT. The measured ΔV_T drops quickly after the stress is removed in GF Planar MOSFET, Comphy could not model this behavior. Comphy needs to be further tested by using higher f AC stress experiments (like BAT [1]) for further verification.

Declaration of competing interest

The authors declare that they have no known competing financial interests or personal relationships that could have appeared to influence the work reported in this paper.

Data availability

The data that has been used is confidential.

References

[1] Mahapatra S. Recent advances in PMOS negative bias temperature instability. Springer Singapore; 2022, http://dx.doi.org/10.1007/978-981-16-6120-4, refer to Ch-4 to Ch-6 for physical BAT framework, Ch-7 to Ch-13 for DC NBTI analysis in multiple device architectures and process conditions, and Ch-14 for AC NBTI analysis.

[2] Pae S, Ashok A, Choi J, Ghani T, He J, hee Lee S, et al. Reliability characterization of 32nm high-k and metal-gate logic transistor technology. In: 2010 IEEE International reliability physics symposium. 2010, p. 287–92. http://dx.doi.org/10.1109/IRPS.2010.5488814.

[3] Ramey S, Ashutosh A, Auth C, Clifford J, Hattendorf M, Hicks J, et al. Intrinsic transistor reliability improvements from 22nm tri-gate technology. In: 2013 IEEE International reliability physics symposium. IRPS, 2013, p. 4C.5.1–5. http://dx.doi.org/10.1109/IRPS.2013.6532017.

[4] Huard V, Ndiaye C, Arabi M, Parihar N, Federspiel X, Mhira S, et al. Key parameters driving transistor degradation in advanced strained sige channels. In: 2018 IEEE International reliability physics symposium. IRPS, 2018, p. P–TX.4–1–P–TX.4–6. http://dx.doi.org/10.1109/IRPS.2018.8353699.

[5] Mitani Y. Influence of nitrogen in ultra-thin SiON on negative bias temperature instability under AC stress. In: IEDM Technical digest. IEEE International electron devices meeting, 2004. 2004, p. 117–20. http://dx.doi.org/10.1109/IEDM.2004.1419082.

[6] Mahapatra S, Goel N, Desai S, Gupta S, Jose B, Mukhopadhyay S, et al. A comparative study of different physics-based NBTI models. IEEE Trans Electron Devices 2013;60(3):901–16. http://dx.doi.org/10.1109/TED.2013.2238237.

[7] Stathis JH, Mahapatra S, Grasser T. Controversial issues in negative bias temperature instability. Microelectron Reliab 2018;81:244–51. http://dx.doi.org/10.1016/j.microrel.2017.12.035.

[8] Mahapatra S, Parihar N. A review of NBTI mechanisms and models. Microelectron Reliab 2018;81:127–35. http://dx.doi.org/10.1016/j.microrel.2017.12.027.

[9] Rzepa G, Franco J, O'Sullivan B, Subirats A, Simicic M, Hellings G, et al. Comphy — A compact-physics framework for unified modeling of BTI. Microelectron Reliab 2018;85:49–65. http://dx.doi.org/10.1016/j.microrel.2018.04.002.

[10] Rzepa G. Comphy code. 2018, URL https://comphy.eu/downloads.

[11] Parihar N, Sharma U, Southwick RG, Wang M, Stathis JH, Mahapatra S. Ultrafast measurements and physical modeling of NBTI stress and recovery in RMG finfets under diverse DC–AC experimental conditions. IEEE Trans Electron Devices 2018;65(1):23–30. http://dx.doi.org/10.1109/TED.2017.2773122.

[12] Parihar N, Goel N, Mukhopadhyay S, Mahapatra S. BTI analysis tool—Modeling of NBTI DC, AC stress and recovery time kinetics, nitrogen impact, and EOL estimation. IEEE Trans Electron Devices 2018;65(2):392–403. http://dx.doi.org/10.1109/TED.2017.2780083.